

# A New Approach to Piezoelectric Shunt Damping

A.J. Fleming, S. Behrens, and S.O.R. Moheimani.  
Department of Electrical and Computer Engineering  
The University of Newcastle, Australia

## Abstract

*Piezoelectric transducer (PZT) patches can be attached to structures in order to reduce vibration. The PZT patches essentially convert vibrational mechanical energy to electrical energy. The electrical energy can be dissipated via an electrical impedance. This paper introduces a method of implementing an arbitrary impedance using a current source and digital signal processor (DSP). The “synthetic impedance” is used to implement a piezoelectric shunt damping circuit for a resonant simply-supported beam.*

## 1 Introduction

Structures such as aircraft and spacecraft experience extensive vibrations during service that can reduce structural life and contribute to mechanical failure. Piezoelectric transducers (PZT’s) in conjunction with appropriate circuitry, can be used as a mechanical energy dissipation device. By placing an electrical impedance across the terminals of the PZT, the passive network is capable of damping structural vibrations. If a simple resistor is placed across the terminals of the PZT, the PZT will act as a viscoelastic damper [5]. If the network consists of a series inductor-resistor  $R - L$  circuit, the passive network combined with the inherent capacitance  $C_p$  of the PZT creates a damped electrical resonance. The resonance can be tuned so that the PZT element acts as a tuned vibrational energy absorber [5]. This damping methodology is commonly referred to as passive shunt damping. Passive shunt damping is regarded as a simple, low cost, light weight, and easy to implement method of controlling structural vibrations. Unlike many active control techniques, passive shunt damping also results in a controlled system that is guaranteed to be stable in the presence of structural uncertainties.

Flexible mechanical structures contain an infinite number of resonant frequencies (or structural modes). If the tuned energy absorber [5] is used to minimize

the vibration of a number of modes, one would need an equal number of PZT patches and shunting circuits. This is clearly impractical. Wu [10] reports a method of damping multiple vibration modes using a single PZT. This circuit includes a “current blocker” comprising of one parallel capacitor-inductor  $C - L$  circuit that is placed in series with each parallel  $R - L$  shunt circuit designed for one structural mode. Depending on the number of structural modes to be shunt damped simultaneously, a different number of  $C - L$  networks are placed in series with the parallel  $R - L$  shunt branch.

There are a number of problems associated with single and multi-mode shunt damping techniques. PZT shunt circuits typically require large inductance values. Therefore, virtual inductors are required to implement the inductor elements. Virtual inductors are large in size and sensitive to component variations and non-ideal characteristics. PZT shunt circuits are capable of generating large voltages for moderate structural excitations. This requires that the virtual inductor circuits be constructed from high voltage operational amplifiers. At least 30 opamps are required to shunt dampen three structural modes<sup>1</sup>.

This paper introduces a method for implementing an impedance of arbitrary order and complexity. This “synthetic impedance” is used in place of shunt damping networks to provide effective structural damping without the problems associated with direct circuit implementations.

## 2 Piezoelectric Devices

Piezoelectric devices have shown promising applications in active, semi-active, and passive vibration control [8]. Piezoelectric materials convert mechanical strains into electrical energy and vice versa. This characteristic can be exploited, allowing them to be used as both sensors and actuators.

---

<sup>1</sup>Based on a series circuit configuration with current blocker’s in every branch, as shown in [10].

## 2.1 Piezoelectricity

Piezoelectricity was discovered by Pierre and Jacques Curie in 1880. It is the phenomenon in which certain crystalline substances develop an electric field when subjected to pressure/forces, or conversely, exhibit a mechanical deformation when subjected to an electric field. This reciprocal coupling between mechanical and electrical energy renders piezoelectric materials useful in many applications including active, semi-active and passive vibration control.

The piezoelectric effect is found only in crystals having no center of symmetry. Examples include quartz, Rochelle Salt and synthetic polycrystalline ceramics; polyvinylfluoride (PVDF) and lead-zirconate-titanate (PZT). The last two are commonly used in vibration control.

The piezoelectric effect is based on the elastic deformation of electric dipoles in a materials crystal lattice. If an external mechanical force deforms the crystal, an electric field and hence a charge distribution at the crystal's surface is generated. This effect is termed the direct piezoelectric or "sensory effect". Applying an electrical field causes a deformation of the dipoles, leading to a constant volume strain of the crystal. This is termed the inverse piezoelectric or "actuator effect".

## 2.2 Piezoelectric Modeling

Piezoelectric crystals have a three-dimensional structure, i.e. crystal deformation occurs in 3 dimensions. Practical mechanical uses only require the effect in one or two dimensions, this can be approximated by manufacturing piezoelectric patches with a large length and width to thickness ratio.

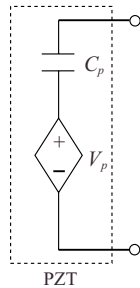


Figure 1: Piezoelectric model.

Piezoelectric transducers behave electrically like a capacitor  $C_p$  and mechanical like a stiff spring [2]. It is common practice to model the piezoelectric element as a capacitor  $C_p$  in series with a voltage source dependent on the dynamics of the resonant structure [4].

An example of the piezoelectric model is shown in Figure 1.

## 3 Piezoelectric Shunt Damping

Shunt damping methodologies are often grouped into two broad categories, single and multi-mode. Single mode shunt damping techniques are simple but damp only one structural mode for every PZT. Multiple mode shunt damping techniques require more complicated shunt circuits but are capable of damping many modes.

### 3.1 Single Mode Shunt Damping

Single mode damping was designed to reduce the magnitude of one structural mode [3, 6]. Two examples of single mode damping are shown in Figure 2, parallel and series shunt damping respectively. Shunting with a  $R - L$  circuit introduces an electrical resonance. This can be tuned to one structural mode in a manner analogous to a mechanical vibration absorber. Single mode damping can be applied to reduce several structural modes with the use of many piezoelectric patches and damping circuits.

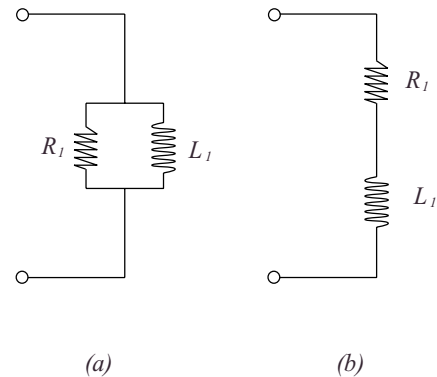


Figure 2: Examples of single mode shunts: (a) parallel case and (b) series case.

Problems may result if these piezoelectric patches are bonded to or imbedded in the structure. First, the structure may not have sufficient room to accommodate all of the patches. Second, if there is insufficient room, the structure may be altered or weakened when the piezoelectric patches are applied. In addition, a large number of patches can increase the structural weight, making it unsuitable for applications such as aerospace.

### 3.2 Multiple Mode Shunt Damping

To alleviate the problems associated with single mode damping, multi-mode shunt damping has been introduced; i.e. the use of one piezoelectric patch to damp several structural modes. There are two common circuit configurations for multi-mode shunt damping, parallel and series. Examples of these two configurations are shown below in Figure 3. There are other examples of multi-mode shunt damping but these will not be discussed in this paper.

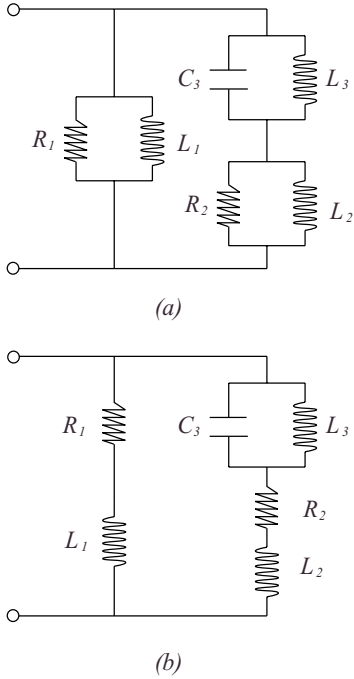


Figure 3: Examples of multiple mode shunts: (a) parallel case [10] and (b) series case.

The principle of multi-mode shunt damping is to insert a current “blocking” circuit [9, 10, 11, 12] in series with each shunt branch. In Figure 3, the “blocking” circuit consists of capacitor and inductor in parallel  $C_3$ - $L_3$ . The number of antiresonant circuits in each  $R$ - $L$  shunt branch depends on the number of structural modes to be shunt damped simultaneously. Each  $R$ - $L$  shunt branch is designed to dampen only one structural mode. For example,  $R_1$ - $L_1$  in Figure 3 is tuned to resonate at  $\omega_1$ , the resonant frequency of the first structural mode to be damped.  $R_2$ - $L_2$  is tuned to  $\omega_2$ , the second structural mode to be damped.

According to [10], the inductance values for the shunt circuits shown in Figure 3 can be calculated from the following expressions. It is assumed that  $\omega_1 < \omega_2$ .

$$L_1 = \frac{1}{\omega_1^2 C_p} \quad (1)$$

and

$$L_2 = \frac{(L_1 \tilde{L}_2 + \tilde{L}_2 L_3 - L_1 L_3 - \omega_2^2 L_1 \tilde{L}_2 L_3 C_3)}{(L_1 - \tilde{L}_2)(1 - \omega_2^2 L_3 C_3)} \quad (2)$$

where  $\tilde{L}_2$  and  $L_3$  are

$$\tilde{L}_2 = \frac{1}{\omega_2^2 C_p} \quad (3)$$

$$L_3 = \frac{1}{\omega_1^2 C_3}. \quad (4)$$

$C_p$  is the capacitance of the PZT.

### 3.3 Implementation Difficulties

Currently shunt damping circuits are implemented using a network of physical components. There are a number of problems associated with this “direct circuit” implementation, the foremost are listed below.

- Typically the shunt circuits require large inductor values (up to thousands of Henries). Virtual grounded inductors and virtual floating inductors (Riordan gyrators [7]) are required to implement the inductor elements. Such virtual implementations are typically poor representations of ideal inductors. They are large in size, difficult to tune, and are sensitive to component age, temperature, and non-ideal characteristics.
- Piezoelectric patches are capable of generating hundreds of volts for moderate structural excitations. This requires the entire circuit to be constructed from high voltage components. Further voltage limitations arise due to the internal gains of the virtual inductors.
- The minimum number of opamps required to implement the shunt damping circuit increases rapidly with the number of modes to be damped. Table 1 summarizes the minimum number of opamps required to implement a series configuration multi-mode shunt damping circuit with current blockers in every branch. The relationship between the number of opamps and the number of modes to be damped for this circuit configuration is given by  $Opamps = 2n + 4n(n - 1)$ , where  $n$  is the number of modes to be damped.

Modes to be damped	Required number of opamps
1	2
2	12
3	30
4	56

Table 1: Number of opamps *vs* number of modes to be damped.

## 4 Implementation of Shunt Damping Circuits

It should be clear from previous sections that although the concept of multi-mode shunt damping is useful, implementation difficulties make its application somewhat limited. This section introduces a new method of implementing the complicated shunt circuit using only a few opamps, one resistor, and a digital signal processor (DSP).

### 4.1 The Synthetic Impedance

We define a “synthetic impedance” as a two terminal device that has an arbitrary relationship between voltage and current at its terminals. The functionality is shown in Figure 4, where:

$$i_z(t) = f(v_z(t)) \quad (5)$$

This can be made to synthesize any network of physical components by fixing  $i_z$  to be the output of a linear transfer function of  $v_z$ . i.e.

$$I_z(s) = Y(s)V_z(s) \quad (6)$$

where  $Y(s) \equiv \frac{1}{Z(s)}$  and  $Z(s)$  is the impedance to be seen from the terminals.

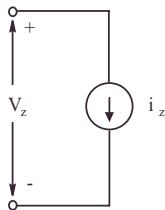


Figure 4: Synthetic impedance functionality.

#### Example 1 *Synthesizing a Series R – L Impedance*

Consider the circuit diagram shown in Figure 5. Suppose that it is desired to synthesize the  $L$  and  $R$

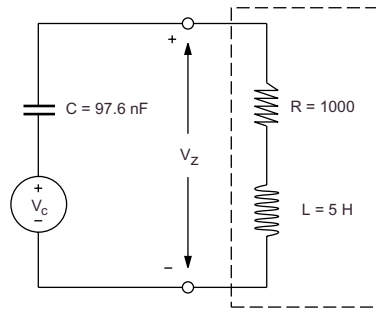


Figure 5: Ideal test circuit.

components. The desired impedance is  $Z_s = Ls + R$ , thus  $Y(s) = \frac{1}{Ls + R}$ .  $Y(s)$  can be implemented using an analog low pass filter with gain or a DSP. In this example the *dSPACE*<sup>2</sup> DSP system is used to simulate the transfer function in real time (any other suitable DSP system may be used). The implementation of the voltage controlled current source is shown in Figure 6. To verify correct operation, the frequency response was measured between the source voltage  $V_c$ , and the synthetic impedance  $V_z$ . This is plotted along with the theoretical response in Figure 7. A more detailed discussion of the implementation follows in later sections.

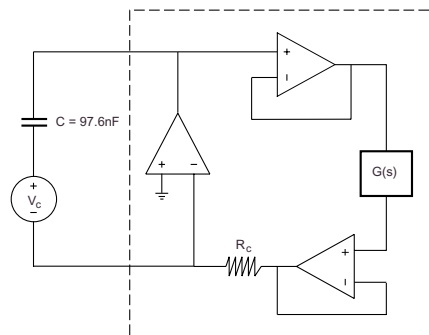


Figure 6: Test circuit with synthetic impedance.

### 4.2 Circuit Diagram / Transfer Function. Interconnection Equivalence

In Example 1,  $Y(s)$  is formed analytically by calculating the complex admittance of the network. In practical situations where there may be a large number of shunt circuit elements, it is desirable to “redraw”

<sup>2</sup>A real time DSP package for prototyping control systems.

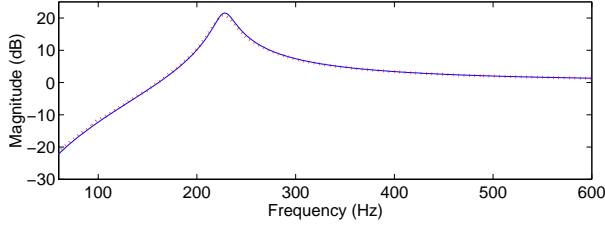


Figure 7: Theoretical (—) and experimental (...) frequency response.

the circuit as a transfer function block diagram so that the overall  $\frac{\text{output}(s)}{\text{input}(s)}$  relationship is equal to  $Y(s)$ . This can simplify the process of writing DSP algorithms. Moreover, if a graphical compilation package such as the Real Time Workshop for MATLAB is available, the need for any transfer function derivations or algorithm coding is completely removed.

Two transformations of interest are shown in Figures 8 and 9. These can be combined to find an equivalent transfer function form for any network of impedances.

**Parallel circuit equivalence.** Consider the parallel network components  $Z_1, Z_2, \dots, Z_i$  as shown in Figure 8. The terminal impedance and admittance of this network is:

$$Z_T(s) = \left( \frac{1}{Z_1} + \frac{1}{Z_2} + \dots + \frac{1}{Z_i} \right)^{-1} \quad (7)$$

$$Y_T(s) = \frac{1}{Z_1} + \frac{1}{Z_2} + \dots + \frac{1}{Z_i} \quad (8)$$

Now consider the transfer function block diagram also shown in Figure 8.

$$G(s) = \frac{T(s)}{R(s)} = \frac{1}{Z_1} + \frac{1}{Z_2} + \dots + \frac{1}{Z_i} \quad (9)$$

It is noted that  $Y_T(s)$  and  $G(s)$  (Equations 8 and 9) are identical. Therefore, if a synthetic impedance (shown in Figure 6) is implemented with a transfer function equal to  $G(s)$ , the impedance seen from the terminals will be identical to the impedance of the parallel network shown in Figure 8 (with impedance  $Z_T(s)$  given by Equation 7).

**Series circuit equivalence.** Consider the series network components  $Z_1, Z_2, \dots, Z_i$  as shown in Figure 9. The terminal impedance and admittance of this network is:

$$Z_T(s) = Z_1 + Z_2 + \dots + Z_i \quad (10)$$

$$Y_T(s) = \frac{1}{Z_1 + Z_2 + \dots + Z_i} \quad (11)$$

Now consider the transfer function block diagram also shown in Figure 9

$$G(s) = \frac{T(s)}{R(s)} = \frac{\frac{1}{Z_1}}{1 + \frac{1}{Z_1}Z_2 + \dots + \frac{1}{Z_1}Z_i} \quad (12)$$

$$G(s) = \frac{1}{Z_1 + Z_2 + \dots + Z_i} \quad (13)$$

It is noted that  $Y_T(s)$  and  $G(s)$  (Equations 11 and 13) are identical. Therefore, if a synthetic impedance (shown in Figure 6) is implemented with a transfer function equal to  $G(s)$ , the impedance seen from the terminals will be identical to the impedance of the series network shown in Figure 9 (with impedance  $Z_T(s)$  given by Equation 10).

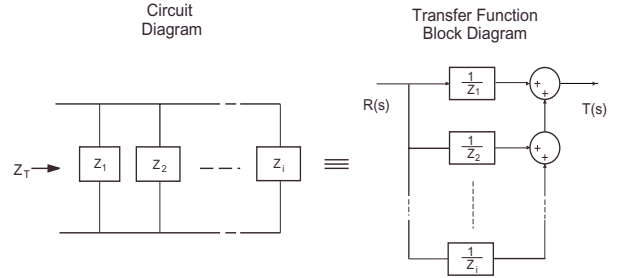


Figure 8: Parallel equivalence.

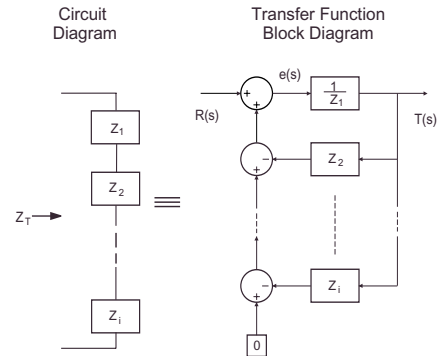


Figure 9: Series equivalence.

## 5 Synthesis of Piezoelectric Shunt Damping Circuits

A synthetic impedance that implements the multi-mode shunt damping circuit shown in Figure 3 (b) will now be designed.

The implementing circuit is shown in Figure 10, this is similar to the example implementation shown in Figure 6. A voltage controlled current source constructed from a single opamp is used together with buffer/amplifiers and a DSP system to simulate an impedance. The two unity gain buffers are replaced with non-inverting amplifiers of gain  $\frac{1}{10}$  and 10. This retains the functionality while allowing the DSP system to operate at a voltage 10 times less than that dealt with by the current source and buffer/amplifiers. A voltage protection device is placed at the input to the DSP analog to digital converter. The only required high voltage components are now the buffer/amplifier and current source opamp. The resistor  $R_c$  sets the transconductance gain of the system. In order to minimize quantization error a reasonable portion of the digital to analog converters range should be utilized. A larger resistor requires a larger voltage to provide a specified current. To maintain a unity transconductance, a gain equal to the value of the resistance  $R_c$  should be placed internally in the DSP algorithm or in series with a transfer function block diagram.

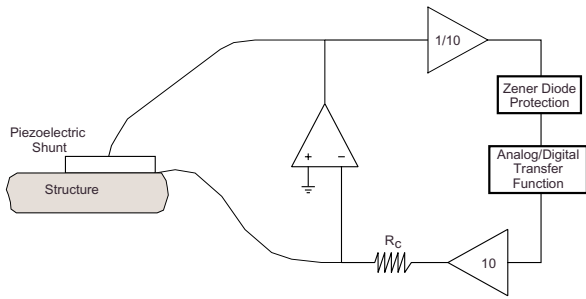


Figure 10: Synthetic impedance implementation.

As discussed in Section 4.2 there are two approaches to designing the DSP algorithm. The first involves deriving the admittance transfer function of the network then implementing the time domain response on the DSP. The second approach, using a graphical compilation package does not require any derivations or coding and will be used here. The circuit of Figure 3 (b) is 'redrawn' in Simulink<sup>3</sup> as a transfer function block diagram using the rules described in Section 4.2. The resulting Simulink block diagram is shown in Figure 11. The Real Time Workshop for Matlab is now invoked to compile the Simulink diagram into executable code. This is downloaded onto the DSP hardware<sup>4</sup> and executed in real time. The sampling time of the digital

<sup>3</sup>A graphical simulation environment for Matlab.

<sup>4</sup>The target processing hardware is the dSPACE ds1103 processing and I/O board.

system is 80 kHz.

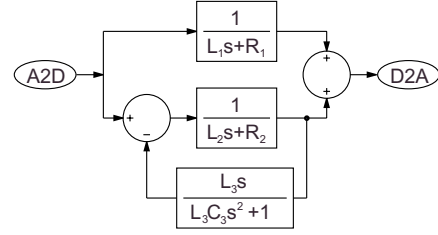


Figure 11: Admittance transfer function.

## 6 Experimental Results

To validate the synthetic impedance, shunt damping experiments were performed on a simply-supported piezoelectric laminated beam, i.e. a mechanically resonant structure. The experimental setup is shown in Figure 12.

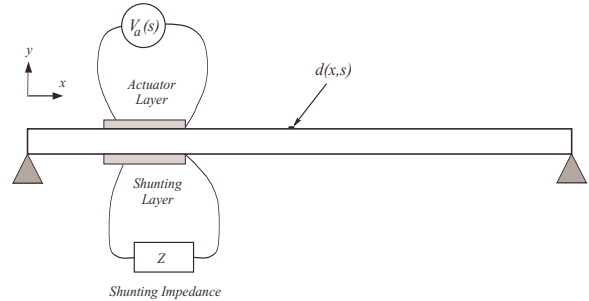


Figure 12: Piezoelectric laminated simply-supported beam.

### 6.1 Experimental Setup

The simply supported beam is a uniform aluminum beam of rectangular cross section with experimentally pinned boundary conditions at both ends. A pair of piezoelectric ceramic patches (PIC151) are attached symmetrically to either side of the beam surface. One patch is used as an actuator and the other as a shunting layer. Experimental beam and piezoelectric parameters are summarized in Tables 2 and 3.

The synthetic impedance is now used in place of the passive network shown in Figure 3 (b). As discussed in Section 5, the circuit is redrawn as a transfer function block diagram then compiled using the MATLAB Real Time Workshop. The resulting DSP application is downloaded and executed on the dSPACE ds1103 DSP board.

Length, $L$	0.6 m
Width, $w_b$	0.05 m
Thickness, $h_b$	0.003 m
Youngs Modulus, $E_b$	$65 \times 10^9 \text{ N/m}^2$
Density, $\rho$	$2650 \text{ kg/m}^3$

Table 2: Parameters of the simply-supported beam.

Length	0.070 m
Charge Constant, $d_{31}$	$-210 \times 10^{-12} \text{ m/V}$
Voltage Constant, $g_{31}$	$-11.5 \times 10^{-3} \text{ Vm/N}$
Coupling Coefficient, $k_{31}$	0.340
Capacitance, $C_p$	0.105 $\mu\text{F}$
Width, $w_s$ $w_a$	0.025 m
Thickness, $h_s$ $h_a$	$0.25 \times 10^{-3} \text{ m}$
Youngs Modulus, $E_s$ $E_a$	$63 \times 10^9 \text{ N/m}^2$

Table 3: Parameters of the PIC151 piezoelectric patches.

Burr-Brown OPA445AP opamps are used in the construction of the current source and buffer/amplifiers, these have a supply voltage limit of  $\pm 45 \text{ V}$ .

The component values for the implemented shunt circuit were derived from Equations (1), (2), (4), and experimentally determined values for  $\omega_1$  and  $\omega_2$ . The capacitance parameter  $C_3$  is arbitrary and is chosen to be  $100 \text{ nF}$ . The resistance values  $R_1$  and  $R_2$  are calculated using the method described in [1]. This method finds resistance values that minimize the  $H_2$  norm of the resulting damped system  $\frac{d(x=0.170,s)}{V_a(s)}$ , where  $d(x,s)$  is the displacement of a point  $x \text{ m}$  from the end of the beam, and  $V_a(s)$  is the applied actuator voltage. A summary of the resulting component values is shown in Table 4.

## 6.2 Results

To examine the damping performance of the synthetic impedance, the piezoelectric actuator is used to

$L_1$	43 H
$L_2$	23.9 H
$L_3$	45.2 H
$R_1$	1543 $\Omega$
$R_2$	1145 $\Omega$
$C_3$	100 nF

Table 4: Component values for the shunt circuit shown in Figure 3 (b).

excite the beam. The frequency response can now be measured between the applied actuator voltage  $V_a(s)$  and the displacement of a point on the beam  $d(x,s)$ . The displacement measurement is performed using a Polytec Scanning Laser Vibrometer (PSV-300). This instrument utilizes the Doppler shift of reflected laser light from a moving target to derive the acceleration, velocity, and displacement of the target.

Figure 13 shows the frequency response of the experimental beam from applied actuator voltage to displacement at a point  $170 \text{ mm}$  from the end of the beam. Both uncontrolled and shunt damped responses are shown.

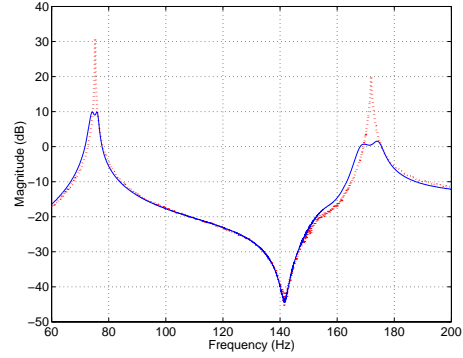


Figure 13: Frequency response of the experimental beam  $\frac{d(x,s)}{V_a(s)}$ . (...) Uncontrolled, (—) Passive damping.

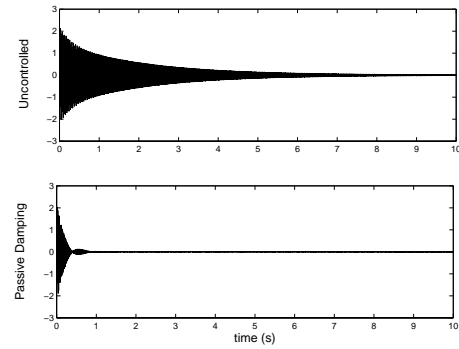


Figure 14: Step response of the experimental beam.

Passive shunt damping using the synthetic impedance results in the second and third structural modes being damped by 22 and 18 dB respectively. A direct circuit implementation of the same shunt circuit, on the same experimental apparatus, results in a peak damping performance of 19.4 and 14.8 dB [1]. It is noted that simulations performed in [1] using ideal

components results in a response that is identical to the that achieved using the synthetic impedance.

Figure 14 shows the uncontrolled and shunt damped step responses of the beam. The input step is bandpass filtered from 40 to 200 Hz, amplified, and applied to the actuator. The velocity at a point 170 mm from the end of the beam is then recorded. The settling time of the shunt damped beam is approximately one eighth that of the uncontrolled beam.

The synthetic impedance has proven to be a high performance method of implementing shunt damping circuits. It has a low number of high voltage components, is virtually immune to sub-optimal performance due to component temperature or time variation, and requires no tuning of sensitive virtual circuits.

## 7 Conclusions

Modern design specifications have given rise to the widespread use of lightweight structures for high performance applications. These structures can be prone to undesirable resonant vibrations. Considerable research has been undertaken with the aim of damping these vibrations using a piezoelectric transducer and shunt damping circuit. Results have been encouraging but the implementation of the damping circuit is impractical due to complexity, component instability, and cost. A method has been presented for synthesizing a network of passive components so that the problems with shunt damping circuits can be alleviated.

The synthetic impedance also provides a means for designing circuit network substitutes with arbitrary response and functionality. Future work may involve using the flexibility of the synthetic impedance to reformulate the damping problem in a control systems perspective.

## References

- [1] S. Behrens and S. O. R. Moheimani. Optimal resistive elements for multiple mode shunt-damping of a piezoelectric laminate beam. Technical Report EE0015, The Department of Electrical and Computer Engineering, The University of Newcastle, March 2000.
- [2] B. Clephas. *Adaptronics and Smart Structures - Basics, Material, Design, and Applications*, chapter 6.2, page 106. Springer, 1999.
- [3] C. M. Fuller et. al. Theoretical and experimental studies of a truss incorporating active members. *Journal of Intelligent Materials Systems and Structures*, 3:333, 1992.
- [4] N. W. Haggood and E. F. Crawley. Experiential investigation of passive enhancement of damping for space structures. *Journal for Guidance, Control and Dynamics*, 14(6):1100, 1991.
- [5] N. W. Haggood and A. Von Flotow. Damping of structure vibrations with piezoelectric materials and passive electrical networks. *Journal of Sound and Vibration*, 14(2):243, 1991.
- [6] J. J. Hollkamp. Multimode passive vibration suppression with piezoelectric materials and resonant shunts. *Journal of Intelligent Materials Systems and Structure*, 5:4, 1994.
- [7] R. H. S. Riodan. Simulated inductors using differential amplifiers. *Electron. Lett.*, 3(2):50–51, 1967.
- [8] K. W. Wang. Structural vibration suppression via parametric control actions - piezoelectric materials with real-time semi-active networks. *Series on Stability, Vibration and Control of Structures*, 1:112–134, 1995.
- [9] S. Y. Wu. Piezoelectric shunts with parallel R-L circuit for smart structural damping and vibration control. *Proceedings of the International Society for Optical Engineering*, 2720:259–269, March 1996.
- [10] S. Y. Wu. Method for multiple mode shunt damping of structural vibration using a single pzt transducer. *Proceedings SPIE: Smart Structure and Materials 1993: Smart Structures and Intelligent System*, 3327:159–168, March 1998.
- [11] S. Y. Wu. Multiple PZT transducer implemented with multiple-mode piezoelectric shunt for passive vibration damping. *Proceedings SPIE: Smart Structures and Materials 1999: Passive Damping and Isolation*, 3672:112–122, March 1999.
- [12] S. Y. Wu and A. S. Bicos. Structure vibration damping experiments using improved piezoelectric shunts. *Proceedings of the International Society for Optical Engineering*, 3045:40–50, March 1997.